1 Introduction

2 Theory

3 Waveguides

In order to understand cavities, we start off with the discussion on waveguides. An electromagnetic wave, when confined to the interior of a hollow pipe is called a waveguide. We shall closely follow the derivation from [1].The generalized Maxwell equations in terms of E-field and H-field are given by:

$$\nabla \times \mathbf{E} = -\frac{\partial B}{\partial t} \tag{3.1}$$
$$\nabla \cdot \mathbf{D} = \rho \tag{3.2}$$
$$\nabla \times \mathbf{H} = \vec{j} + \frac{\partial D}{\partial t} \tag{3.3}$$
$$\nabla \cdot \mathbf{B} = 0 \tag{3.4}$$

In vacuum, these equations become:

$$\nabla \times \mathbf{E} = \mu_0 \cdot \frac{\partial H}{\partial t} \tag{3.5}$$
$$\nabla \cdot \mathbf{E} = 0 \tag{3.6}$$
$$\nabla \times \mathbf{H} = \epsilon_0 \cdot \frac{\partial E}{\partial t} \tag{3.7}$$
$$\nabla \cdot \mathbf{H} = 0 \tag{3.8}$$

Upon solving these equations, we get plane wave solutions which looks like this:

$$\Delta\vec{E}\left(\vec{r}\right) + \frac{\omega}{c^2}\vec{E}\left(\vec{r}\right) = 0$$
$$\Delta\vec{B}\left(\vec{r}\right) + \frac{\omega}{c^2}\vec{B}\left(\vec{r}\right) = 0$$

Now, let us look at a waveguide which is aligned along the z-direction. Taking the ansatz $\vec{E} = \vec{E}(x, y).e^{i(\omega t - kz)}$ and the separation $\Delta = \Delta_\perp + \frac{\partial^2}{\partial z^2}$, for the longitudinal fields yields:

$$\Delta_\perp E_z + k_c^2 E_z = 0 \tag{3.9}$$
$$\Delta_\perp H_z + k_c^2 H_z = 0 \tag{3.10}$$

where

$$k_c^2 = \frac{\omega^2}{c^2} - k^2$$

The quantity k_c is called the critical wave number and is a characteristic property of the cavity, as we shall see. Solving these equations further, we see that it is sufficient to know the longitudinal fields, E_z and B_z because we can easily determine the transverse components from them.

$$ik_c^2\vec{E}_\perp = k\vec{\nabla}_\perp E_z + \omega\mu_0\vec{\nabla}_\perp H_z \times \hat{e}_z \tag{3.11}$$
$$ik_c^2\vec{H}_\perp = k\vec{\nabla}_\perp H_z - \omega\epsilon_0\vec{\nabla}_\perp E_z \times \hat{e}_z \tag{3.12}$$

Now, there are two waves to classify these waves:

1. $k_c^2 = 0$
   (a) $\vec{\Delta}_\perp E_z \neq 0$ and $\vec{\Delta}_\perp H_z \neq 0$: HE or EH hybrid waves.
   (b) $\vec{\Delta}_\perp E_z = 0$ and $\vec{\Delta}_\perp H_z = 0$: TEM waves.
2. $k_c^2 \neq 0$ In this case we do not get any propagation if $\omega \leq c \cdot k_c$. These waves are called evanescent waves or the cut off condition. The possible propagation modes are:

(a) $E_z = 0$: TE (transversal electric) or H waves.

(b) $H_z = 0$: TM (transversal magnetic) or E waves.

Corresponding to this critical wave, we have a critical frequency, which is $\omega_c = k_c.c$, below which there is no propagation. One interesting thing to note here is that for a hollow waveguide, only TE or TM modes are possible, TEM is not, because no wave would exist in this case [1]. But for a coaxial cable, which consists of straight wire surrounded by a conduction sheath, we can get TEM modes.

3.1 Cylindrical waveguides

We now consider a cylindrical waveguide with an inner radius a. This imposes the following boundary conditions to the walls of the waveguide:

- $E_\phi = 0$, $E_z = 0$ for $r = a$
- $H_r = 0$ for $r = a$

The field distribution solution for a cylindrical waveguide can be separated into angular and radial parts, whose solutions are then given by the Bessel/Neumann functions. These can be then substituted in the eq.(3.11)-(3.12) and upon imposing the constraints from the boundary condition gives us the corresponding TE- and TM-modes.

3.2 Cylindrical waveguides resonator

The time has now come, to talk about cavities itself. If we now insert two conducting plates perpendicular to the z-axis, the incoming wave is reflected completely, giving us standing waves. Because of this, the z-dependence changes like:

$$a \cdot e^{ikz} \implies A \cdot \sin(kz + \phi_0)$$

The following condition is imposed so that the longitudinal boundary conditions are fulfilled: $k = p \cdot \pi/l$. The longitudinal field looks like:

$$\begin{aligned}
\mathbf{TE_{mnp} - Modes} &: H_z = H_{mn} \cdot J_m(k_c r)\cos(m\phi) \cdot \sin(p\pi/l \cdot z) \cdot e^{\omega_{mnp} t};\\
&\quad \text{where } k_c a = j'_{mn}\\
\mathbf{TM_{mnp} - Modes} &: E_z = E_{mn} \cdot J'_m(k_c r)\cos(m\phi) \cdot \cos(p\pi/l \cdot z) \cdot e^{\omega_{mnp} t};\\
&\quad \text{where } k_c a = j_{mn}
\end{aligned}$$

For resonant frequency, we have:

$$\omega_{mnp} = c \cdot \sqrt{(j_{mn}/a)^2 + (p\pi/l)^2}$$

Here, J_m is the m-th Bessel function, J'_m is its derivative. And j_{mn} and j'_{mn} are the n-th zeropoints of the m-th Bessel function and its derivative.
The resonant modes can be written in the linear form as:

$$(d\nu)^2 = \left(\frac{c j^{(')}_{mn}}{\pi}\right)^2 + \left(\frac{c}{2}\right)^2 p^2 \left(\frac{d}{l}\right)^2 \tag{3.13}$$

here d is the diameter of the cavity. When we plot different modes on a graph, we get a mode map (Fig.3.1). The mode map allows one to read off the resonant frequencies for different diameters and length of the cavity.
Since the derivative of the zeroth order Bessel function and the first order Bessel function, j'_{0n} and j_{1n}, are equal, the corresponding TE- and TM-modes have the same resonant frequencies. That is, TE_{0np}-modes and TM_{1np}-modes have the same resonant frequency.

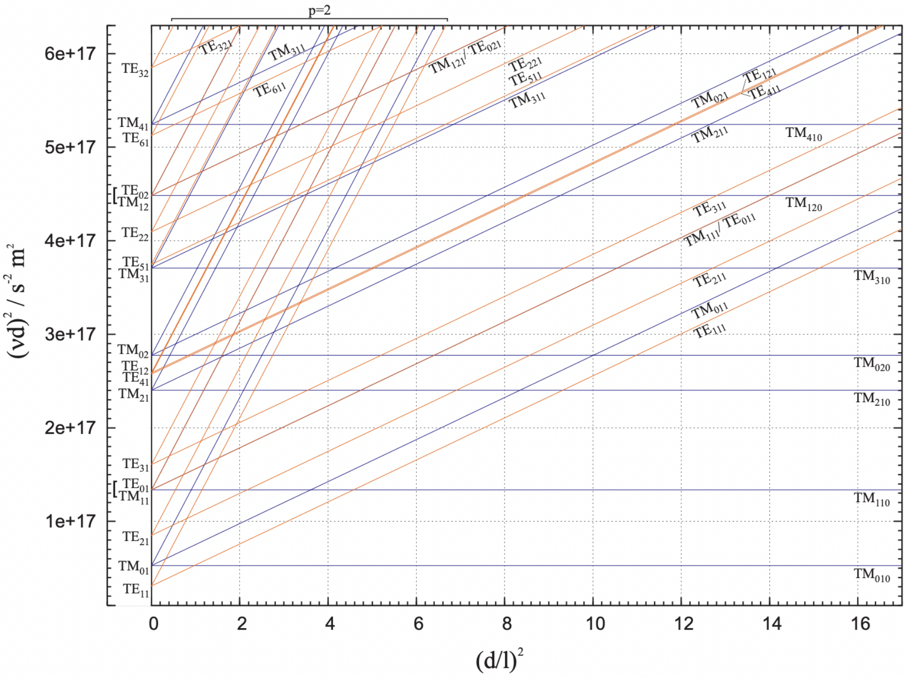

Figure 3.1: Mode map for $p \leq 2$. [1]

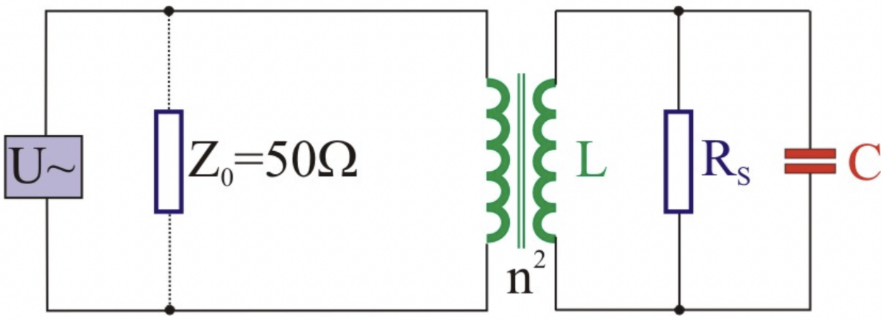

Figure 4.1: Equivalent circuit of a cavity with loop coupling. [1]

4 Oscillating circuit

A cavity has a lot of characteristic quantities, which can be described by an equivalent circuit (Fig.4.1). Coupling is a process through which electromagnetic waves can be coupled to a waveguide, or in this case, to a cavity. There are several ways to couple and in this experiment, we use loop coupling, which enables coupling to the magnetic field inside the cavity. In the figure 4.1, the LCR-circuit represents the cavity. The step-down transformer represents the loop coupling, Z_0 is the characteristic impedance and R_s is the Shunt impedance.
The characteristic quantities associated with the cavity are:

- Quality factor
- Coupling coefficient
- Reflection coefficient
- Shunt impedance

Let us look at these quantities in a bit more detail.

4.1 Quality factor

Quality factor is a dimensionless quantity which describes how underdamped an oscillator or resonator is. It is defined as:

$$Q_0 = \frac{2 \cdot \pi \text{stored energy}}{\text{losses per period}} = \frac{2\pi \cdot W}{T \cdot P} = \frac{\omega_0 \cdot W}{P} \tag{4.1}$$

where ω_0 is the angular resonant frequency. Looking at the case of driven oscillations, the unloaded quality factor can be determined from the Full Width Half Maximum (FWHM), $\Delta\omega_H$

$$Q_0 = \frac{\omega_0}{\Delta\omega_H} \tag{4.2}$$

4.2 Coupling coefficient

The coupling coefficient is defined as:

$$\kappa = \frac{Z_a}{Z_0} = \frac{R_s}{n^2 Z_0} = \frac{Q_0}{Q_{ext}} \tag{4.3}$$

where n is the transformer turn ratio, Q_0 is the unloaded quality factor and Q_{ext} is the external quality factor. If we know the coupling coefficient, the unloaded quality factor can be calculated using:

$$\frac{1}{Q} = \frac{1}{Q_0} + \frac{1}{Q_{ext}}$$

$$Q_0 = (1 + \kappa) \cdot Q \tag{4.4}$$

We also get 3 cases for the coupling coefficient, which are:

- $\kappa < 1$: undercritical coupling, $Q > Q_0/2$
- $\kappa = 1$: critical coupling, $Q = Q_0/2$ (no reflection)
- $\kappa > 1$: overcritical coupling, $Q < Q_0/2$

4.3 Reflection coefficient

In the conductor, we have an incoming wave $(\hat{U}_+, \hat{I}_+)$ and reflected wave $(\hat{U}_-, \hat{I}_-)$. Hence we define the complex reflection coefficient as:

$$\rho = \frac{\hat{U}_-}{\hat{U}_+} \tag{4.5}$$

The coupling coefficient and the reflection coefficient are related at resonance by:

$$\kappa = \left| \frac{1+\rho}{1-\rho} \right| \tag{4.6}$$

We shall discuss more about this in the next section.

4.4 Shunt impedance

Shunt impedance tells us how much energy is gained by a charged particle when it crosses the cavity. It is defined by:

$$R_s = \frac{U^2}{2P_V} = \frac{1}{P_V} \left| \int_{L/2}^{-L/2} E_0(s) \cdot e^{i\omega_0 s/c} \cdot ds \right|^2 \tag{4.7}$$

The impedance of the resonator in fig.4.1 is a complex quantity. This value only becomes real at resonance and when it does, it is called the Shunt impedance. This value is typically of the order of 10^6 Ω. This is the reason we use a step down transformer in the circuit, using loop coupling, as seen in Eq.(4.3).

5 Scalar measurement of reflection coefficient

The reflection coefficient we defined in the previous section (eqn. 4.5) is a complex value. It looks like:

$$\rho(\Delta\omega) = \rho_0(\Delta\omega) \cdot e^{-2ikl} = \frac{\kappa - \left(1 + 2iQ_0 \frac{\Delta\omega}{\omega}\right)}{\kappa + \left(1 + 2iQ_0 \frac{\Delta\omega}{\omega}\right)} \cdot e^{-2ikl}$$

We get this when we investigate only take $\Delta\omega \ll \omega_0$. When this reflection coefficient is measured some distance l away from the cavity, we get the delay factor of e^{-2ikl}.

Now, we can separate the real and imaginary part and get its modulus:

$$|\rho(\Delta\omega)| = |\rho_0(\Delta\omega)| = \sqrt{\frac{(\kappa-1)^2 + 4Q_0^2\left(\Delta\omega/\omega\right)^2}{(\kappa+1)^2 + 4Q_0^2\left(\Delta\omega/\omega\right)^2}} \tag{5.1}$$

The scalar network analyzer should then look like fig. 5.1.

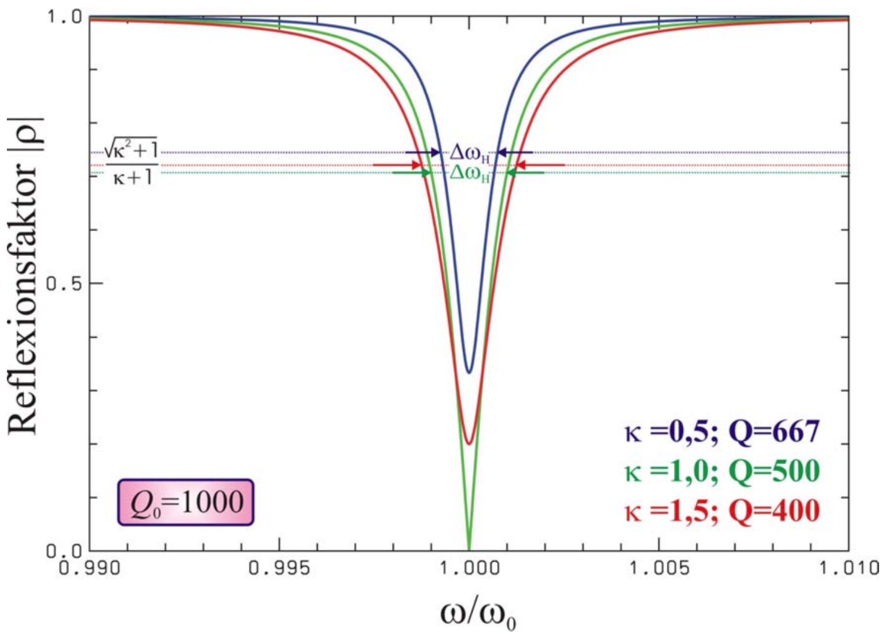

Figure 5.1: Reflection coefficient for different values of coupling coefficient and Quality factors along with FWHM ($\Delta\omega_H$). [1]

From the figure, we can see that the reflection is minimum at resonance. At resonance, the value of the reflection coefficient is given by:

$$|\rho(\Delta\omega = 0)| = \left|\frac{\kappa - 1}{\kappa + 1}\right| \tag{5.2}$$

The equation can be inverted to calculate the value of coupling coefficient. But one cannot distinguish between $\rho > 0$ and $\rho < 0$.
In order to calculate the value of reflection coefficient at FWHM, we use the following relation (which one can derive by using eqn.(4.2), (4.4) and (5.1):

$$|\rho(\Delta\omega_H/2)| = \frac{\sqrt{\kappa^2+1}}{\kappa+1} \tag{5.3}$$

It is important to note that only the case of $\kappa = 1$ do we get the FWHM at $\rho = 1/\sqrt{2}$. This is because of the way we define dB-values, which will be discussed in another section.
In all other cases,

$$|\rho(\Delta\omega_H/2)| = \frac{\sqrt{\kappa^2+1}}{\kappa+1} \neq \frac{1}{\sqrt{2}}$$

6 Vectorial measurement of reflection coefficient

The vectorial reflection coefficient is given by:

$$\rho(\Delta\omega) = \frac{(\kappa-1)^2 - 4Q_0^2\left(\Delta\omega/\omega\right)^2 - 4i\kappa Q_0 \Delta\omega/\omega}{(\kappa+1)^2 + 4Q_0^2\left(\Delta\omega/\omega\right)^2} \cdot e^{-2ikl} \tag{6.1}$$

Neglecting the delay coefficient term, e^{-2ikl}, we get an equation, which when plotted on the complex plane (close to the resonance), ρ_0 describes a circle of radius r around (x_0, y_0). The radius r is given by:

$$r = \frac{\kappa}{1+\kappa}$$

We find that all the positions of circles are independent of quality factor and depend only on the coupling coefficient. Another interesting thing we find is that all these circles go through (-1, 0) (as shown in fig. 6.1).

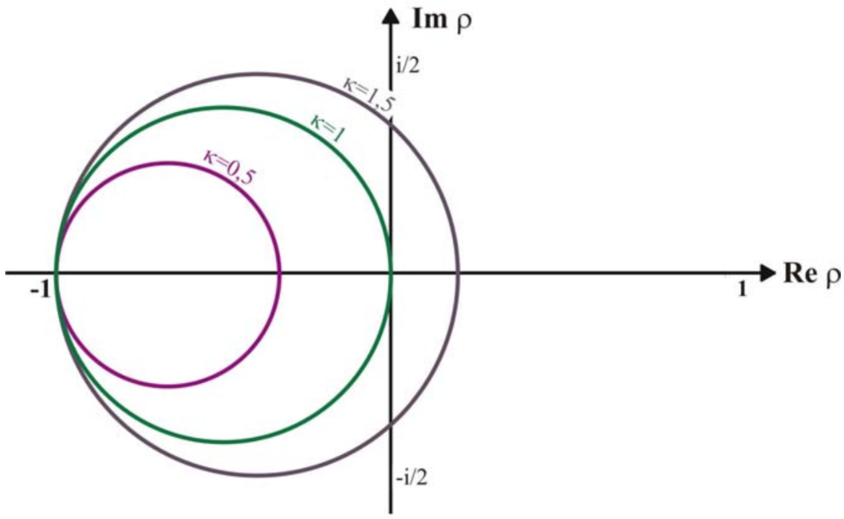

Figure 6.1: Different position and radii for different values of κ. [1]

Now taking the delay coefficient into account, we see the circles rotate around the origin (fig. 6.2). For large values of quality factor, the distortion in the shape of the circle is negligible, but it is quite noticeable in low values of quality factor. We will be neglecting these distortions in our measurements because we such calibrations can be done only on expensive equipments.
In fig. 6.2, we also notice that we have an outer circle which is the reflection circle. It represents complete reflection of frequencies far away from the resonance one. The smaller circle is called the resonance circle.

6.1 Determining resonant frequency and coupling

7 Experimental Setup

In our experiment, we used three cylindrical cavities, each with a length of $L_{cav} = 20\,\text{mm}$ with an inner diameter of $d_{cav} = 78.5\,\text{mm}$. The first and second cavity are completely sealed and are free to move, but differ in their coupling position to the radio frequency. The third cavity is open from the sides and is mounted on a rail, in which its position can be freely adjusted and is displayed on an external device digitally. The cavities used are shown in Fig. 7.1.
To measure the resonant frequencies, reflection coefficients, and other relevant quantities in our experiment, we utilize a Vector Network Analyzer (VNA) shown in Fig. 7.2. The VNA generates a signal from its AC source and it is transmitted through the coaxial cable connected to the ports of the VNA. The resulting transmission or reflection of the signal is then shown on the display as a function of the frequency of the signal (in Hz). The units displayed can be altered between U, the ratio between output and input signal, and $dB = 20\log_{10}(U)$.

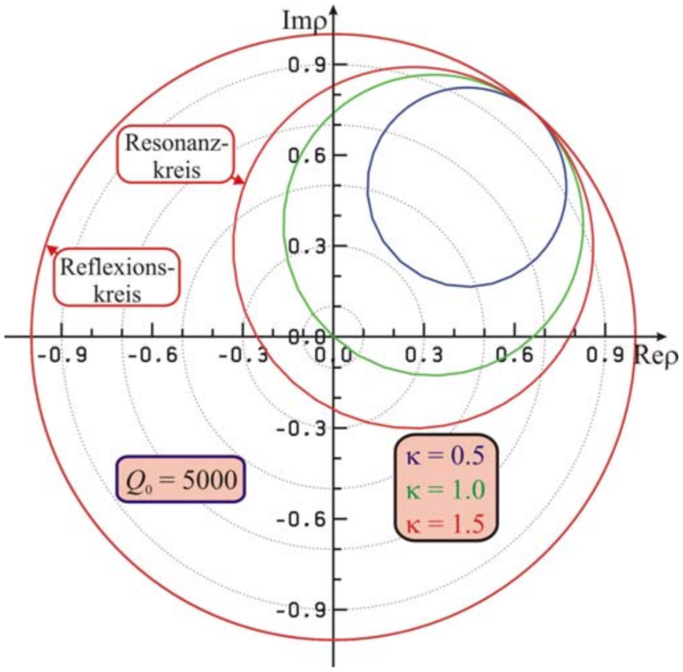

Figure 6.2: The delay coefficient rotates the circle around the origin. We can also see the Resonance and Reflection circle. [1]

(a)

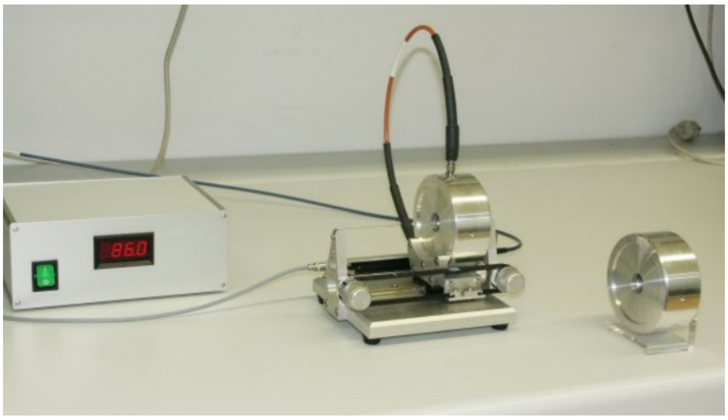

(b)

Figure 7.1: The three cavities used in this experiment. (a): The cavity with top coupling. The connector that couples the radio frequency can be observed. (b) The cavity with side coupling (right) and the mounted cavity (left) [1]. The detector used to measure the position of the mounted cavity is also shown.

8 Procedure

8.1 Attenuation and Reflection in Coaxial Cables

As the coaxial cable connects the cavity to the VNA, we need to choose a cable such that it does not interfere with the measurement of the cavity's response. To determine the optimal coaxial cable to use, we thus measured the attenuation and reflection of different coaxial cables at different frequency ranges. In our experiment, this was done for the RG-142 and ST-18 cables with a length of $l_{RG142} = 51.02 \pm 0.10\,\mathrm{cm}$ and $l_{ST18} = 182.55 \pm 0.10\,\mathrm{cm}$ respectively.

To measure the attenuation and reflection, we first calibrated the VNA to the silver RG402 coaxial cable with a length of $l_{RG402} = 30.02 \pm 0.01\,\mathrm{cm}$. The calibration process was performed using a full-two port calibration with the TOSM algorithm provided by the VNA. The open, short, and load (with termination

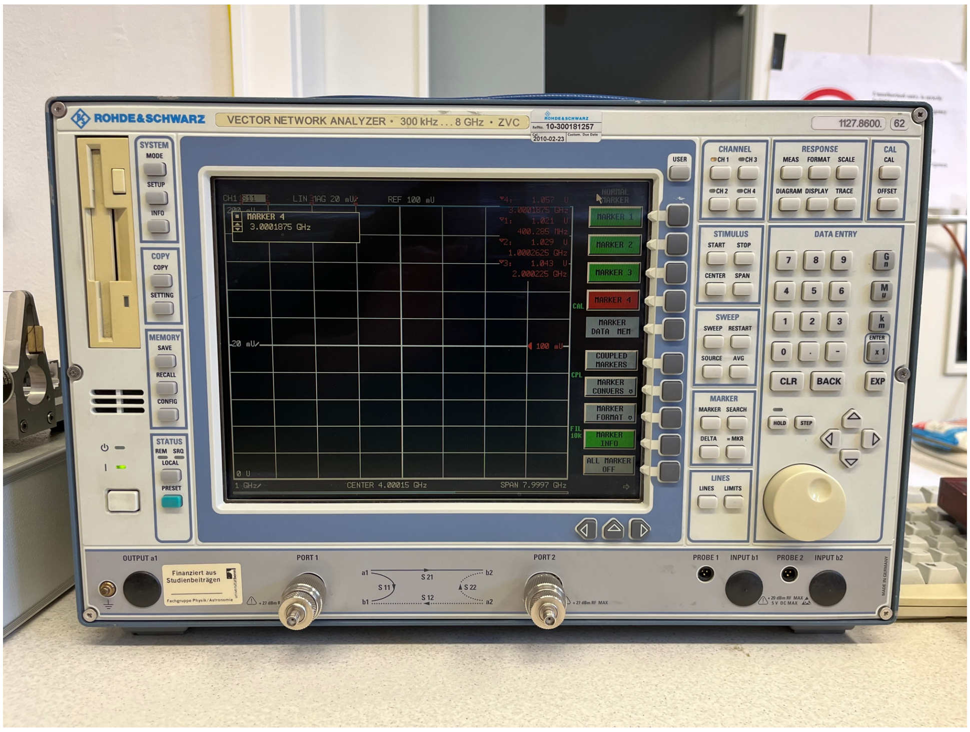

Figure 7.2: The Rhode & Schwarz Vector Network Analyzer used in this experiment.

impedance of 50 Ω) at the two ports (port 2 on the VNA and the coaxial cable) were then calibrated by utilizing the provided calibration kit (Fig. 8.1).
The attenuation of the signal was then measured by connecting the end of the coaxial cable to the input port (port 2) on the VNA. We then connect the same load from the calibration kit to the end of the coaxial cable to measure the reflection coefficient. Both measurements were performed to verify that the VNA was properly calibrated.
After the calibration was performed with the silver cable, we connected the two coaxial cables to the silver cable and measured their attenuation and reflection coefficient by performing the same procedure as with the silver one. The raw measurements obtained are shown in Fig. 8.2 and Fig. **??**. The value at several frequencies were tabulated (and were used to determine the attenuation of the cable. The attenutation was the compared to those from given datasheets).

References

[1] Michael Switka. *E106 Cavities Assignments and details of procedure and analysis*. Mar. 2022.

Figure 8.1: The open (left), short (middle) and load (right) used for calibration in this experiment.

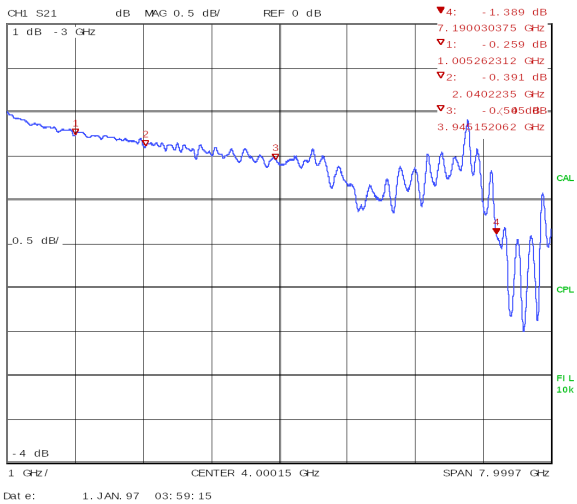

(a) Attenuation for the RG142 cable.

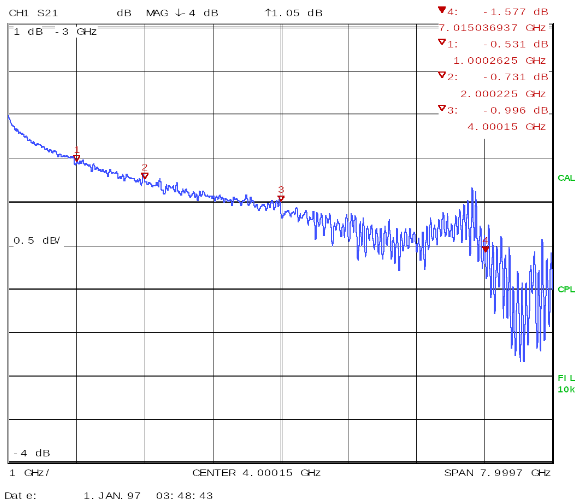

(b) Attenuation for the ST18 cable.

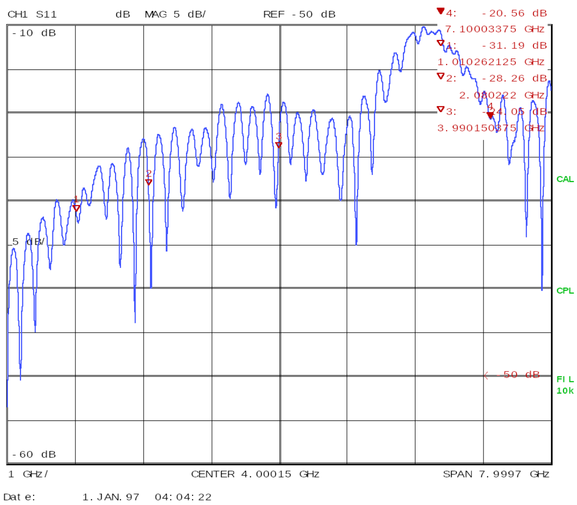

(c) Reflection for the RG142 cable.

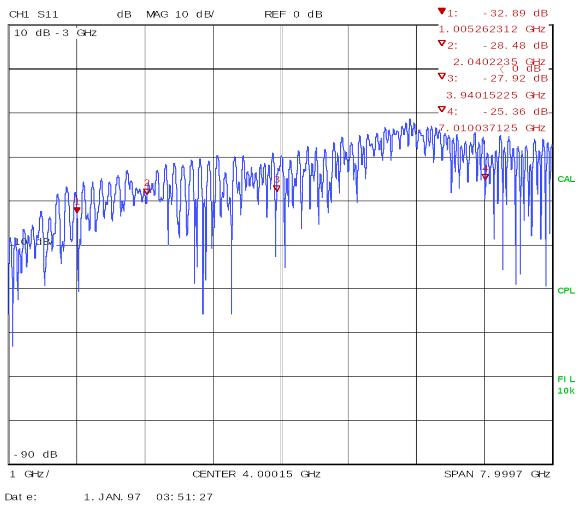

(d) Reflection for the ST18 cable.

Figure 8.2: The attenuation and reflection for the RG142 and ST18 coaxial cables. The values at several frequencies are also shown on the top right of each figure.